Characterization of the radiative properties of homogeneous, anisotropic or non homogeneous porous media

Jean Taine, Franck Enguehard

Characterization of the radiative properties of homogeneous, anisotropic or non homogeneous porous media

Jean Taine and Franck Enguehard*
Laboratoire EM2C(UPR288 CNRS),
CentraleSupélec
Bat. Péclet, Grande Voie des Vignes
92295 Chatenay-Malabry, France.
jean.taine@ecp.fr; franck.enguehard@ecp.fr

September 2015

1 Introduction

Radiation transfer plays a determinant role in applications at high temperature, in particular in porous media. The field of applications is wide. In catalytic combustion or catalytic reforming, the interfaces of the porous medium are covered by a catalyzer: The use of a porous medium allows lower temperature conditions and consequently a minimization of pollutants generation. Porous media are also used in solar absorbers, waste combustion, etc. The degraded core of a nuclear reactor is, at the beginning of a severe accident, a large-scale porous medium in which radiative transfer is determinant. Another class of applications deals with the walls of engines and rockets under thermodegradation. This list is not exhaustive.

As it is not realistic to completely study heat transfer within a porous medium from pore scale, a homogenization of the medium is necessary. Whatever the type of real phase, a homogenized phase is, from the radiation point of view, a semi transparent medium, even for a medium with opaque and transparent phases. In most of the studies, this homogenization step has been carried out by empirical methods based on two assumptions:

- The homogenized phase follows the Beer's law, *i.e.* exponential extinction law;

- The phase function which plays an important role in porous media, generally characterized by strong back scattering, is assumed to follow an imposed law, for instance of Henyey-Greenstein type[1].

Indeed, the classical homogenization methods are generally based on a parameter identification technique. This technique (see for instance Refs.[2, 3, 4, 5, 6, 7, 8, 9]) is based on entry data issued from experimental determination, in some particular conditions, or on a set of numerical data issued from radiative transfer calculations. Uncertainties due to experiments or radiative model, to the limitations of the imposed physical laws and to the identification technique in use are then cumulated. This method, based on a large number of parameters to be determined, generally allows to fit all these parameters, which have or do not have a physical meaning, even

*The authors acknowledge for outstanding contributions Estelle Iacona and Fabien Bellet, their colleagues of ECP, Dr Florian Fichot HDR (IRSN), Drs Manuel Tancrez, Barbar Zeghondy, Elie Chalopin, Miloud Chahlafi, Vincent Leroy and Marie Zarrouati, former PhD students of ECP, and Yann Dauvois, PhD student of ECP. These works have also been partially supported by Gaz de France, IRSN, Air Liquide, CEA-DAM and ECP.

for instance when the Beer's law is not valid. A detailed review of these techniques is given in Ref.[10].

In fact a large number of porous media are not Beerian. It is the case of statistically non homogeneous media[11], of statistically homogeneous but anisotropic media[12, 13] and even of statistically isotropic and homogeneous media. For instance, a homogeneous and isotropic medium of DOOS type (Dispersed Overlapping Opaque Spheres within a transparent phase) is always Beerian, but a medium of DOTS type (Dispersed Overlapping Transparent Spheres within an opaque phase, practical model of foams) is never exactly Beerian: The Beer's law is less and less verified when the medium porosity decreases. In practice, the Beer's law is not valid for a porosity smaller than 0.6[14]. Consequently, the physical validity of the Beer's law has to be checked before any radiative transfer study in a porous medium.

Due to the intense recent development of the tomography techniques, the morphology of many real porous media is now known with a high spatial resolution. Only statistical methods allow the huge number of data issued from these experiments to be applied to radiation modeling. An original statistical approach for characterizing the radiative properties of a homogenized phase of a porous medium has been developed, initially by Tancrez and Taine[14]. Many other works based on these approaches have been published in the last decade[11, 12, 13, 15, 16, 17, 18, 19, 20].

In this statistical approach, extinction, absorption and scattering properties of a homogenized phase are directly, completely and accurately, characterized by radiative statistical distribution functions, instead of three scalars, *i.e* extinction, absorption and scattering coefficients: These quantities have a physical meaning only in the case of a Beerian homogenized phase. As the whole radiative distribution functions are accurately known, the Beerian assumption can be accurately validated or, often, not validated. Moreover a general scattering phase function, depending on both the incidence and scattering directions, is directly determined only from the physical laws assumed at local scale.

An important assumption of the method is that the geometrical optics laws are valid: The typical radiation wavelengths have to be shorter than the typical pore scale. The necessary morphology data are obtained from either γ or X tomography techniques at a spatial resolution a, or exactly in the case of classical models (overlapping or not overlapping spheres or finite cylinders, etc.) Moreover, radiation properties of the porous medium are assumed known at a scale smaller than a: Reflection law in the case of an opaque phase; Reflection and transmission laws at interfaces, absorption, scattering coefficients and phase function if a real semi transparent phase is involved.

Section 2 is devoted to the development of the physical model for any type of porous medium, Section 3 to the determination of the radiative statistical functions, based on a Monte Carlo method, Section 4 to some key properties of a medium at equilibrium, which are used in the modeling of emission and scattering in the companion paper[21]. Different models of radiative transfer are studied in this paper.

2 Physical model

2.1 Radiative statistical functions

2.1.1 General case

The radiative effective properties of a homogenized phase of a porous medium, possibly statistically anisotropic and non homogeneous, *i.e* non Beerian, are exhaustively characterized by

four statistical functions. These quantities are defined along any axis of direction $\mathbf{u}(\theta, \varphi)$ and coordinate s (see Fig.1):

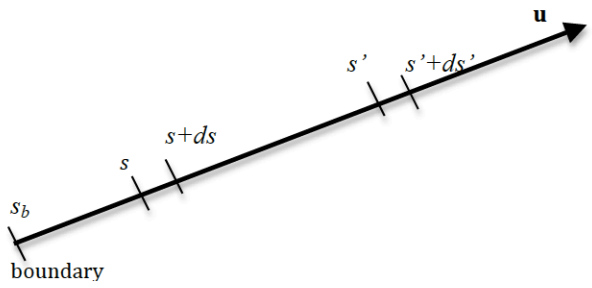

Figure 1: Coordinates

i) An *extinction cumulative distribution function* $G_{ext\,\nu}(s, \mathbf{u}, s' - s)$, which is in fact the cumulative distribution function of the lengths $s' - s$ of all the intervals MI joining any point M of abscissa s in the direction $\mathbf{u}$, within the considered phase, to the associated extinction point I of abscissa s'. I can belong to the core of the phase, if it is semi transparent at local scale, or can be, in any case, an impact point at the interface with another phase. It is worth noticing that $1 - G_{ext\,\nu}(s, \mathbf{u}, s' - s)$ simply is the transmissivity $\tau_\nu(s, \mathbf{u}, s' - s)$ of the homogenized phase in the direction $\mathbf{u}$.

ii) An *absorption cumulative probability* $P_{a\,\nu}(s, \mathbf{u}, s' - s)$, which is the probability that a ray issued from a point $M(s)$ of a phase in the direction $\mathbf{u}$ is absorbed within this phase or at an opaque interface before a distance $s' - s$ from M,
or

iii) A *scattering cumulative probability* $P_{sc\,\nu}(s, \mathbf{u}, s' - s)$, which is the probability that a ray issued from a point $M(s)$ of a phase in the direction $\mathbf{u}$ is scattered within this phase or at an interface before a distance $s' - s$ from M; $P_{sc\,\nu}(s, \mathbf{u}, s' - s)$ is linked to the previous quantities by

$$G_{ext\,\nu}(s, \mathbf{u}, s' - s) \;=\; P_{a\,\nu}(s, \mathbf{u}, s' - s) \;+\; P_{sc\,\nu}(s, \mathbf{u}, s' - s). \tag{1}$$

Note that, in the common case of a porous medium with a transparent phase and an opaque solid phase of diffuse gray absorptivity α, $P_{a\,\nu}(s, \mathbf{u}, s' - s)$ and $P_{sc\,\nu}(s, \mathbf{u}, s' - s)$ are simply equal to $\alpha\, G_{ext}(s, \mathbf{u}, s' - s)$ and $(1 - \alpha)\, G_{ext}(s, \mathbf{u}, s' - s)$, respectively.

IVi) A *general phase function* $p_\nu(s, \mathbf{u_1}, \mathbf{u})$, depending in the general case on the incidence and scattering directions, respectively characterized by $\mathbf{u_1}$ and $\mathbf{u}$.

2.1.2 RDFI method: Validity of the Beerian approximation

Note that, in the particular case of a Beerian medium, case of many statistically homogeneous and isotropic porous media, the radiative statistical functions $G^B_{ext\,\nu}$, $P^B_{a\,\nu}$ and $P^B_{sc\,\nu}$ are simply exponential. For instance, the whole extinction cumulative distribution function

$$G^B_{ext\,\nu} \;= 1 \;-\; \exp[-\beta_\nu\,(s' - s)] \tag{2}$$

is completely characterized by a scalar, extinction coefficient β_ν. Similarly, the whole absorption and scattering probabilities $P^B_{a\,\nu}$ and $P^B_{sc\,\nu}$ are completely defined by the absorption coefficient

κ_ν and the scattering coefficient σ_ν, with: $\beta_\nu = \kappa_\nu + \sigma_\nu$.

A statistically non homogeneous medium is never Beerian. Moreover, after homogenization, a phase of a porous medium is not rigorously Beerian, in most cases. This property is exactly verified only for singular geometrical configurations, for instance between overlapping or non overlapping spheres or cylinders, but not within these spheres or cylinders. Nevertheless, a medium can be, in many cases, considered as approximately Beerian and characterized by optimized values of the extinction, absorption and scattering coefficients in a given range of optical thickness.

The method of Radiative Distribution Function Identification (RDFI) is based on a criterion of validity of the Beerian assumption[14, 15], from an accurate determination of the radiative statistical functions, in particular of G_{ext}. A homogenized phase can approximately be considered as Beerian if the Beerian extinction cumulative distribution function $G^B_{ext\,\nu}$ associated with the optimal fitted value of the extinction coefficient β_ν^{RDFI} fulfills the following condition *in the optical thickness range* [0, 3]

$$\epsilon_{ext}(\beta_\nu(\mathbf{u})) = \left(\sum_{i=1}^{N} [G_{ext\,\nu}(\mathbf{u}, v_i) - G^B_{ext\,\nu}(\mathbf{u}, v_i)]^2 / \sum_{i=1}^{N} [1 - G_{ext\,\nu}(\mathbf{u}, v_i)]^2 \right)^{1/2} < \eta, \qquad (3)$$

where N discrete values v_i of $s' - s$ are used. A typical value of η is 0.04. The real behavior of G_{ext}, for such a medium, is discussed in Sec.4.1.2.

Note that, in most of the other methods, the Beerian assumption is used without justification.

2.2 Radiative Intensity

For the sake of simplicity, the developments of this Section are limited to a porous medium with an Opaque solid phase and a Transparent fluid phase (OT). The other cases will be systematically studied in the companion paper[21].

Consider, around a point M, an elementary volume $\mathrm{d}V$ of the whole porous medium, typically an elementary cylinder of cross-section $\mathrm{d}S$ and length $\mathrm{d}s$. The fraction per unit volume of the homogenized phase, which occupies the volume of the transparent propagation phase, is Π. Emission and scattering which occur within $\mathrm{d}V$, in an elementary solid angle $\mathrm{d}\Omega$ around the direction $\mathbf{u}$, generate a radiative flux in this direction: $[S_{sc\,\nu}(s, \mathbf{u}) + S_{e\,\nu}(s, \mathbf{u})]\,\mathrm{d}V\,\mathrm{d}\Omega\,\mathrm{d}\nu$. In this expression, $S_{sc\,\nu}(s, \mathbf{u})$ and $S_{e\,\nu}(s, \mathbf{u})$ *respectively are the scattering and emission source terms in the direction* $\mathbf{u}$*, per unit volume* $\mathrm{d}V = \mathrm{d}S\,\mathrm{d}s$ *of the whole porous medium and consequently are proportional to* Π. Under the previous assumptions, the intensity I_ν in the direction $\mathbf{u}$ within the homogenized phase at a point $M'(s')$ is simply expressed as (see Fig.1)

$$\begin{aligned} I_\nu(s', \mathbf{u}) &= \int_{s_b}^{s'} [S_{sc\,\nu}(s, \mathbf{u}) + S_{e\,\nu}(s, \mathbf{u})]\,\tau_\nu(s, \mathbf{u}, s' - s)\,\mathrm{d}s + \Pi\, I_{b\,\nu}(\mathbf{u})\,\tau_\nu(s_b, \mathbf{u}, s' - s_b) \\ &= \int_{s_b}^{s'} [S_{sc\,\nu}(s, \mathbf{u}) + S_{e\,\nu}(s, \mathbf{u})]\,[1 - G_{ext\,\nu}(s, \mathbf{u}, s' - s)]\,\mathrm{d}s \\ &+ \Pi\, I_{b\,\nu}(s_b, \mathbf{u})\,[1 - G_{ext\,\nu}(s_b, \mathbf{u}, s' - s_b)], \end{aligned} \qquad (4)$$

where $\Pi\, I_{b\,\nu}(s_b, \mathbf{u})$ is the intensity leaving the boundary of the porous medium in the direction $\mathbf{u}$, at the abscissa $s_b(\mathbf{u})$, within the homogenized phase (which explains the factor Π). This intensity depends on the environment of the porous medium and can be expressed from the classical laws of radiative transfer. Note that the intensities $I_\nu(s', \mathbf{u})$ and $I_{b\,\nu}$ in the previous equation possibly include a refractive index.

The scattering source terms have different origins: i) Scattering by a real semi transparent phase of the porous medium; ii) Reflection at an interface with another phase; iii) Transmission at an interface between two semi transparent phases or between semi transparent and transparent ones. Whatever the type of scattering, the expression of the scattering source term $S_{sc\,\nu}(s,\mathbf{u})$, detailed in Ref.[20, 22], is given by the following equation of which the spatial and directional quantities are defined in Fig.2

$$\begin{aligned} S_{sc\,\nu}(s',\mathbf{u}) &= \int_{4\pi}\int_{s_{1b}}^{s'_1} \frac{\mathrm{d}P_{sc\,\nu}}{\mathrm{d}v}(s_1,\mathbf{u}_1,s'_1-s_1)\,\frac{p_\nu(\mathbf{u}_1,\mathbf{u})}{4\pi}\,[S_{sc\,\nu}(s_1,\mathbf{u}_1)+S_{e\,\nu}(s_1,\mathbf{u}_1)]\,\mathrm{d}s_1\,\mathrm{d}\Omega_1 \\ &+ \int_{4\pi} \frac{\mathrm{d}P_{sc\,\nu}}{\mathrm{d}v}(s_{1b},\mathbf{u}_1,s'_1-s_{1b})\,\frac{p_\nu(\mathbf{u}_1,\mathbf{u})}{4\pi}\,\Pi\,I_{b\,\nu}(s_{1b},\mathbf{u}_1)\,\mathrm{d}\Omega_1, \end{aligned} \tag{5}$$

in which $\Pi\,I_{b\,\nu}(s_{1b},\mathbf{u}_1)$ is the intensity leaving the boundary of the porous medium in the direction $\mathbf{u}_1$, at the abscissa $s_{1b}(\mathbf{u}_1)$, within the homogenized phase.
Note that the scattering occurs within all elementary volume $\mathrm{d}V$. The same point M' is characterized by the abscissa s' in the considered direction $\mathbf{u}$ and by an abscissa s'_1 in the current direction $\mathbf{u}_1$ of a ray before its scattering around the point M'. Consequently, the boundaries of the elementary volume are s' and $s'+\mathrm{d}s'$ in the direction $\mathbf{u}$, and $s'_1+\mathrm{d}s'_1$ in the direction $\mathbf{u}_1$. These notations are used along both this paper and its companion[21].

$\frac{\mathrm{d}P_{sc\,\nu}}{\mathrm{d}v}(s_1,\mathbf{u}_1,s'_1-s_1)\,\mathrm{d}s'_1$, where v is equal to s'_1-s_1, is the probability for the energy associated with the total source term $S_{sc\,\nu}(s_1,\mathbf{u}_1)+S_{e\,\nu}(s_1,\mathbf{u}_1)$, in s_1, in $\mathrm{d}\Omega_1$ around the direction $\mathbf{u}_1$, to be scattered between s'_1 and $s'_1+\mathrm{d}s'_1$; $\frac{p_\nu(\mathbf{u}_1,\mathbf{u})}{4\pi}\,\mathrm{d}\Omega$ is the probability to be scattered in $\mathrm{d}\Omega$, around the direction $\mathbf{u}$. In cases i) and ii) the radiation is scattered in the same medium as the incident one. On the contrary, in case iii) the initial and final media are generally characterized by different values of the refractive index.

The emission source term $S_{e\,\nu}(s_1,\mathbf{u}_1)$ strongly depends on the scales at which the temperature field is defined compared to the scales of the radiative properties. Its expression will be detailed in the companion paper: Its modeling depends on the thermal conditions of the system and on the modeling of other heat transfer modes.

2.3 Generalized Radiative Transfer Equation; Memory effect

The commonly encountered homogenized phases that do not follow the Beer's law cannot be modeled, in a general case, by using a classical Radiative Transfer Equation (RTE): Indeed, extinction, absorption and scattering coefficients have then no more physical meaning. For this type of non Beerian phases, a Generalized Radiative Transfer Equation (GRTE) has been introduced by Taine et al.[20]. It is directly expressed in terms of the radiative statistical functions instead of the extinction, absorption and scattering coefficients. This equation, one of the most implicit ones of the physics, will only be briefly commented here; It simply writes, in case ii)

$$\begin{aligned} \frac{\mathrm{d}I_\nu}{\mathrm{d}s'}(s',\mathbf{u}) = &- \int_{s_b}^{s'} [S_{sc\,\nu}(s,\mathbf{u})+S_{e\,\nu}(s,\mathbf{u})]\,\frac{\mathrm{d}G_{ext\,\nu}}{\mathrm{d}s'}(s,\mathbf{u},s'-s)\,\mathrm{d}s \\ &- \Pi\,I_{b\,\nu}(\mathbf{u})\frac{\mathrm{d}G_{ext\,\nu}}{\mathrm{d}s'}(s_b,\mathbf{u},s'-s_b) + S_{sc\,\nu}(s',\mathbf{u})+S_{e\,\nu}(s',\mathbf{u}). \end{aligned} \tag{6}$$

In the other cases the GRTE must account for multiple extinction and source terms (see the companion paper[21]).

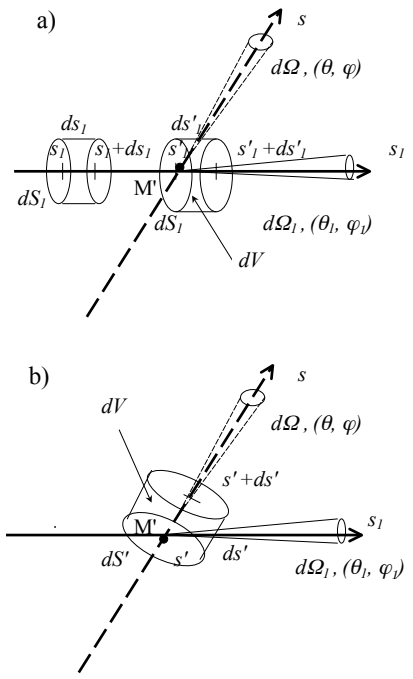

Figure 2: Scattering source term: a) dV is defined by reference to the coordinates of the direction $\mathbf{u}_1$; b) by reference to the coordinates of the direction $\mathbf{u}$.

The first member of Eq.6 is a classical transport term, practically always considered in steady state. In other cases, at extremely short time scales for instance, an unsteady term $\frac{1}{c}\frac{\partial I_\nu}{\partial t}$ is added to this term.

The first term of the second member of the GRTE is an extinction term. It is worth noticing that it cannot be expressed in terms of the intensity! Indeed, the components of the intensity, issued from different points s, are submitted to different extinction phenomena, depending on $G_{ext\,\nu}(s, \mathbf{u}, s'-s)$. Consequently, the knowledge of the intensity is not sufficient for characterizing extinction: There is a "memory effect" for each elementary radiation beam. It is only for Beerian media that the variation of the intensity dI_ν, due to local absorption and scattering, can be determined from the knowledge of this local intensity I_ν. Indeed, the proportionality of dI_ν to I_ν is the definition property of an exponential function.

The second term of the second member simply is the extinction term of the intensity issued from the boundary s_b of the porous medium.

The two last terms of the second member are the source terms associated with scattering and emission by $[s', s' + \mathrm{d}s']$ in the direction $\mathbf{u}$.

The formalism associated with the GRTE could seem complex. In fact, the GRTE can be numerically solved as easily as a classical RTE by a stochastic Monte Carlo method: Indeed, it is directly expressed in terms of cumulative distribution functions, which is the first requirement of a Monte Carlo method.

3 Radiative properties determination

The radiative statistical functions can only be defined within Representative Volumes (RV). These representative volumes are extremely various. They are generally built by using the possible macroscopic symmetries and periodicities of the porous medium. The typical dimensions of a RV can be characterized by small, intermediate or large optical thicknesses, depending on the macroscopic morphology of the medium. The representativity has to be checked by comparing the results associated with different zones of the porous medium. Some examples are given in the following.
Note that these radiative RVs are not similar to the REVs in use in many porous media models. Indeed, the radiative statistical functions are defined at a scale which is much smaller than the REV size (see Sec.4 of the companion paper[21]).

The position and the shape of an elementary volume $\mathrm{d}V$ of the whole real porous medium is not modified after homogenization. But, contrary to the case of the real medium, the homogenized phase, considered as an effective semi transparent medium, is continuous. It is characterized, within the elementary volume $\mathrm{d}V$, by a *presence probability* which is its fraction per unit volume Π, *i.e.* the porosity in the case of a fluid phase. Consequently, *the propagation phase is assumed to be present in any point*, at this probabilistic sense. A determinant advantage of the method is to be based on the whole radiative distribution functions, that cover all the spatial scales, from optically thin scales to optically thick scales. Consequently, after homogenization the vicinity of any point is representative of all the medium: the homogenization is not based on averaged values as in most of other methods.

3.1 General assumptions

In all this study, the geometrical optics laws are assumed valid : The radiation wavelength is small compared to the typical sizes of the considered structures.

The morphology of the real medium is assumed known, exactly in the case of regular structures (bundles of rods[12], set of overlapping or not overlapping spheres[14, 11] or finite cylinders[23], etc.), or from high resolution γ[13] or X[15] tomography of spatial resolution a.

A key assumption is that the radiative properties of the real phases at local scale, *i.e* at a scale smaller than a, are known: Complete reflectivity law for an opaque interface, extinction, absorption and scattering coefficients, phase function and refractive index for a semi transparent real phase.

3.2 Statistically homogeneous medium

In most cases, the medium is considered as statistically homogeneous but often statistically anisotropic and non Beerian. In case of strong porosity gradients, in particular in the vicinity of a wall, a more advanced model dedicated to statistically non homogeneous porous media is developed in Sec.3.3.

3.2.1 Medium with an opaque phase and a transparent one (OT)

a) Determination of G_{ext} and p_ν

This case is frequently encountered, typically with a solid phase and air as propagation phase. Within the real medium, extinction only occurs when a ray, issued from any point of the transparent phase, hits an opaque interface. Radiation is then partially absorbed and partially reflected, as shown in Fig3. These surface phenomena become volume phenomena within the

homogenized propagation phase: Extinction, absorption and scattering in a continuous semi transparent medium. They are characterized in a general case by $G_{ext}(s, \mathbf{u}, s'-s)$, $P_{a\,\nu}(s, \mathbf{u}, s'-s)$ and $P_{sc\,\nu}(s, \mathbf{u}, s'-s)$ and a general phase function $p_\nu(s, \mathbf{u_1}, \mathbf{u})$. As the extinction of rays issued

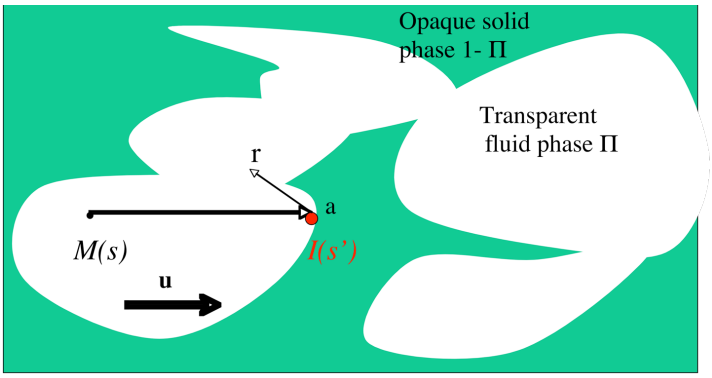

Figure 3: Principle of G_{ext} determination (OT case)

from any points M of the propagation phase only occurs at points I of the interface, as shown in Fig.3, the cumulative extinction distribution function $G_{ext}(s, \mathbf{u}, s'-s)$ is equal to the cumulative distribution function of the lengths of the segments MI, that is a purely geometrical quantity, which is *independent of the radiation frequency, i.e.*

$$G_{ext}(s, \mathbf{u}, s'-s) = \frac{1}{\Pi\,\delta V}\frac{1}{\delta\Omega}\int_s^{s'}\int_{\Pi\,\delta V}\int_{\delta\Omega}\delta[s''-s_0(\mathbf{r},\mathbf{u})]\,\mathrm{d}\Omega(\mathbf{u})\,\mathrm{d}\mathbf{r}\,\mathrm{d}s''. \tag{7}$$

In Eq.7, the summations are carried out on a discretized elementary volume $\Pi\delta V$ of the transparent phase of the real medium, around the point $M(\mathbf{r})$, in a discretized elementary solid angle $\delta\Omega$, around the direction $\mathbf{u}$; s is the abscissa of M in the direction $\mathbf{u}$ and, for a given couple $(\mathbf{r}, \mathbf{u})$, s_0 is the abscissa of the associated impact point I; δ is the Dirac distribution.

G_{ext} is determined by a numerical Monte Carlo method. A huge number of shots are issued from random points of the transparent phase within a given Representative Volume (RV) when the real medium presents many symmetries, or within a large number of samples of the medium when it is not the case.[1] The distances MI associated to all the shots allow G_{ext} to be built step by step[14].

For each shot, a random number r in the range $[0, 1]$ is compared to the absorptivity value $\alpha_\nu(\mathbf{n}, \mathbf{u})$, where the normal unit vector $\mathbf{n}$ associated with an impacting ray is defined by both the source point $M(\mathbf{r})$ and the incidence direction $\mathbf{u}$. $P_{a\,\nu}$ or $P_{sc\,\nu}$ are then incremented for $r < \alpha_\nu(\mathbf{n}, \mathbf{u})$ or $r > \alpha_\nu(\mathbf{n}, \mathbf{u})$, respectively[14, 15, 13].

In the considered OT case, the expression of the phase function $p_\nu(\mathbf{u_1}, \mathbf{u})$ is deduced from the bidirectional reflectivity $\rho''_\nu(\mathbf{u_1}, \mathbf{u}, \mathbf{n}(\mathbf{r}, \mathbf{u}_1))$, that exhaustively characterizes the reflection law at an opaque interface. The incidence and scattering directions $\mathbf{u_1}$ and $\mathbf{u}$ are defined *in a fixed frame associated with the whole porous medium* and not in the local frame associated with

[1] Note that only scattering, absorption and extinction are accounted for in the characterization of the radiative properties of a phase of a porous medium. It is not the case of emission, of which the modeling also strongly depends on the temperature field properties. Consequently, the origin points of the shots, within the real medium, belong to all the volume of the propagation phase and not only, in the case of opaque interfaces, to interfaces which emit and scatter radiation. This approach is validated by its results: For instance, the behaviors of the extinction cumulative distribution functions at both the optically thin and the optically thick limits, which can be theoretically predicted (see the following Sections), are exactly found.

the normal at any impact point. Finally, p_ν writes

$$\mathrm{d}\Omega_1 \left(\frac{p_\nu(\mathbf{u_1}, \mathbf{u})}{4\pi} \, \mathrm{d}\Omega \right) = \left(\frac{\mathrm{d}\Omega_1/(\Pi\, V) \int_{\Pi,\, V \,/\, \mathbf{u}.\mathbf{n} \geq 0} \rho''_\nu \left[\mathbf{u_1}, \mathbf{u}, \mathbf{n}\,(\mathbf{r}, \mathbf{u}_1)\right] \left[-\mathbf{u_1}.\mathbf{n}\,(\mathbf{r}, \mathbf{u}_1)\right] \, \mathrm{d}\mathbf{r}}{\int_{4\pi} 1/(\Pi\, V) \int_{\Pi\, V \,/\, \mathbf{u}'.\mathbf{n} \geq 0} \rho''_\nu \left[\mathbf{u_1}, \mathbf{u}', \mathbf{n}\,(\mathbf{r}, \mathbf{u}_1)\right] \left[-\mathbf{u_1}.\mathbf{n}\,(\mathbf{r}, \mathbf{u}_1)\right] \, \mathrm{d}\mathbf{r}\, \mathrm{d}\Omega'} \right) \mathrm{d}\Omega. \quad (8)$$

In this equation, the condition $\mathbf{u}.\mathbf{n} \geq 0$ expresses that a scattered ray does not go through the opaque phase. In practice, ρ'' is not experimentally known in a given application. A specular or a diffuse reflection law is generally used; Sometimes, a linear combination of these laws. The determination of the phase function is detailed in Appendices A and B.

Within the same Monte Carlo calculations, random numbers in the range $[0, 1]$, shot in the reflection cumulative distribution function (the bidirectional reflectivity), allow the two angles defining the scattering direction $\mathbf{u}(\theta, \phi)$ to be determined. ρ'' is often a joined cumulative distribution function of θ and ϕ. The general phase function $p_\nu(\mathbf{u_1}, \mathbf{u})$ is then directly built from the assumed reflection law, without any other assumption. More details are given, for instance, in Refs.[14, 12, 13].

Due to the huge number of shots, the determination of G_{ext}, $P_{a\,\nu}$, $P_{sc\,\nu}$ and p_ν is very accurate, as shown in the following examples.

b) Examples of geometrically defined media

The first study of Tancrez and Taine[14] has been devoted to models of foams: Sets of Dispersed size Overlapping Transparent Spheres within an opaque medium (DOTS) and Dispersed size Overlapping Opaque Spheres within a transparent medium (DOOS), following a terminology of Torquato[24]. Each realization of the medium is carefully and numerically built in order to validate both statistical homogeneity and isotropy of the medium. For each of the 10^4 statistical realizations of the medium, 10^2 shots are issued from a cubic shot zone enclosed in a cubic study zone, such that practically all shots are extinguished within this zone.

If the extinction cumulative distribution functions associated with DOOS are rigorously exponential, those associated with DOTS are approximately Beerian for high porosity values, but strongly deviate from exponential functions when the porosity decreases, as shown in Fig.4, even if the medium is statistically homogeneous and isotropic. Indeed, $\ln(1 - G_{ext})$ should be a straight line. Note that all curves associated with different values of the porosity Π present:

- A slope at origin $-\beta_{OT}$, where β_{OT} is an extinction coefficient, only defined at the *optically thin limit*[14] and expressed in the following. This case corresponds to weak $\beta_{OT}(s' - s)$ values.

- Linear asymptotic behaviors, for large $\beta_{OT}(s' - s)$ values (*optically thick limit*), but characterized by different slopes. A precise physical explanation of this last fact will be given in Sec.4.1.2

These behaviors at the optically thin and thick limits can be observed for all porous media. In the present case of a statistically homogeneous and isotropic medium, the value of the slope at the optically thin limit can be simply found. Whatever the reflection law at the opaque interface, this interface is characterized by an hemispherical absorptivity α^h_ν and the absorption coefficient κ_ν is given by[14]: $\kappa_\nu = \alpha^h_\nu\, \beta$, where β is the extinction coefficient. If the medium is Beerian (it is the case at the optically thin limit), the flux emitted by the real interfaces, of area $\mathrm{d}S$, belonging to an optically thin elementary volume $\mathrm{d}V$ of the porous medium, without self-absorption, is $\alpha^h_\nu\, \mathrm{d}S\, \pi I^\circ_\nu(T)$; The same flux emitted by the corresponding homogenized phase is: $\kappa_\nu\, \Pi\, \mathrm{d}V\, 4\pi I^\circ_\nu(T)$. Consequently: $\kappa_\nu = \alpha^h_\nu\, (\mathrm{d}S \,/\, 4\,\Pi\, \mathrm{d}V)$ and the extinction coefficient at the optically thin limit is then, for any statistically homogeneous and isotropic medium: $\beta_{OT} = (A/\,4\,\Pi)$, where A is the specific area of the porous medium $\mathrm{d}S/\mathrm{d}V$. As in Fig.4 the

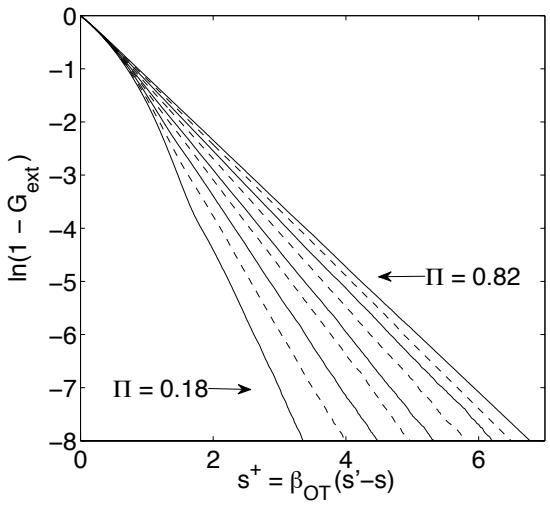

Figure 4: G_{ext} associated with DOTS vs porosity for the same value of the specific area per unit volume of the fluid phase A/Π[14], cited in [20]; $\beta_{OT} = A/(4\Pi)$: extinction coefficient for an optically thin medium; $\Pi = 0.18$, 0.26, 0.37, 0.48, 0.56, 0.65, 0.72, 0.78, 0.82

results are plotted for the same value of the specific area per unit volume of the fluid phase A/Π, a common slope of the curves equal to $-\beta_{OT}$ is observed.
Results associated with diffuse and specular reflection laws have been systematically studied vs Π in Ref.[14]. For this statistically homogeneous and isotropic medium, the obtained corresponding phase functions depend only on the scattering angle cosine.

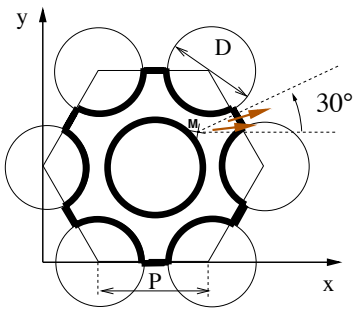

Figure 5: Triangular configuration. Cross-section of the shooting and studied zone. A perfect specular reflection ($\rho = 1$) is applied at any impact at a symmetry plane.

Another case of perfectly defined geometrical configuration is a bundle of rods of an intact nuclear reactor core. Both triangular (see Fig.5) and square configurations have been studied[12, 20]. This medium is periodical, statistically homogeneous but strongly anisotropic: G_{ext} depends both on the angle θ with the rod axes and on the azimuth φ. The calculations are only carried out:
- In a plane cross-section of the system ($\theta = \pi/2$): MI lengths associated with any θ values are easily deduced from these results. Moreover, due to the periodicity of the triangular configuration, for instance, the shooting and studied zone is simply the void phase included in the hexagon connecting adjacent rod axes (see Fig.5);
- For φ values in the range [0, 30°], due to the symmetries of the system.

Examples of strong variations of $G_{ext}(\theta = \pi/2,\, \varphi)$ vs φ are given in Fig.6. All curves converge at the optically thin limit to the value[12] $-\beta_{OT} = -\frac{A}{\pi\,\Pi}$ associated with this configuration. When it is non truncated, each of them converges, as in the previous case, to an asymptotic straight line (optically thick limit).

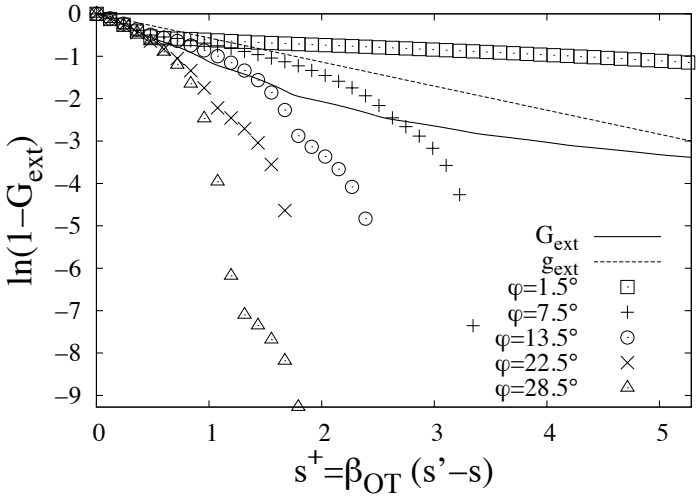

Figure 6: $G_{ext}(\theta = \pi/2, \varphi)$ vs $\beta_{OT}(s' - s) = \frac{A}{\pi\,\Pi}(s' - s)$; G_{ext} is averaged over all φ values; g_{ext} is the associated Beerian best fit; $\Pi = 0.750$ [20].

c) Media defined from tomography data

Chahlafi et al.[13] have studied the same type of rod bundles, but extracted from the cen-

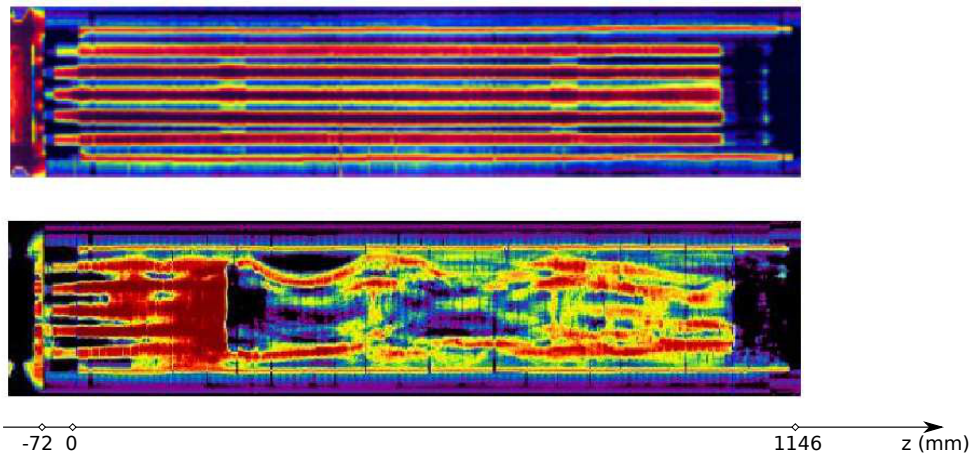

Figure 7: Axial cross-sections along z-axis of an intact bundle (above) and a degraded one (below) of Phebus FPT1 experiments [25, 13].

tral region of a nuclear core, where they have locally been submitted to the conditions of a severe accident (experiments FTP1 of CEA/IRSN[25]): The morphology of a degraded rod bundle has been studied by γ tomography. A spatial reference is required for defining the cutoff in density levels issued from tomography experiments, associated with the interfaces between

opaque walls and the transparent medium. The study of an intact bundle has allowed this cutoff criterion to be determined. Examples of intact and degraded rod bundles are shown in Fig.7.

A set of quasi homogeneous transverse zones, characterized by quasi uniform Π and A values has been determined. For each zone, as previously, calculations have been carried out in transverse cross-sections ($\theta = \pi/2$), more precisely in the same shooting and studied zone as for the intact system, accounting for all its symmetries. Examples of homogeneous but strongly anisotropic and non Beerian extinction cumulative distribution functions are shown in Fig.8. As the general phase function is extremely complex to show, the scattering asymmetry factor

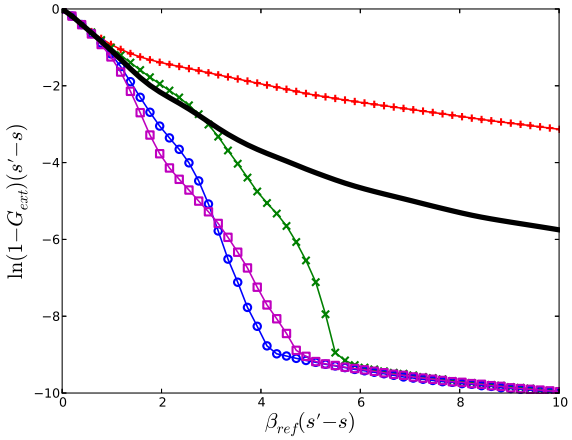

Figure 8: Extinction cumulative distribution function $G_{ext}(\theta = \pi/2, \varphi)$ of a zone; Squared configuration; From above to below: $\varphi = 1.5°$ (red crosses); $\varphi = 16.5°$ (green crosses); $\varphi = 31.5°$ (blue circles); $\varphi = 43.5°$ (violet squares); G_{ext} for all φ values (thick line).

$g(\theta, \varphi)$ defined by

$$g(\theta, \varphi) = \frac{1}{4\pi} \int_0^{\pi} \int_0^{2\pi} (\mathbf{u}_1.\mathbf{u})\, p_\nu(\theta_1, \varphi_1, \theta, \varphi)\, \mathrm{d}\Omega_1 \tag{9}$$

has been plotted in Fig.9

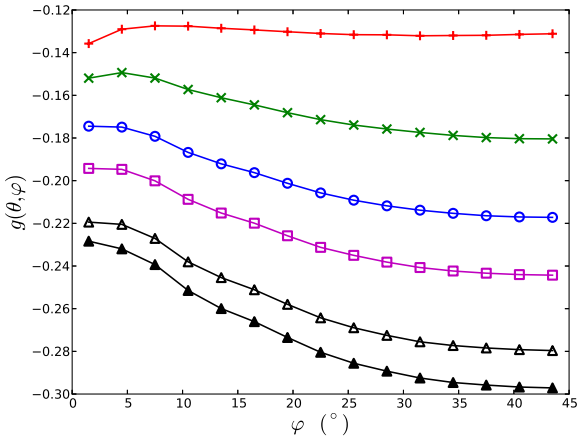

Figure 9: Scattering asymmetry factor $g(\theta, \varphi)$ of a zone; Squared configuration; From above to below: $\theta = 14°$; $\theta = 34.1°$; $\theta = 44.9°$; $\theta = 53.9°$; $\theta = 69.3°$; $\theta = 90°$.

3.2.2 Medium with an opaque phase and a semi transparent one (OST)

The same rod bundles filled with a mixture of water vapor and water droplets at high pressure have been studied in Ref.[13] for application to the reflooding of a degraded nuclear core at the beginning of a severe accident.
The radiative properties of the medium without semi transparent phase are characterized by $G_{ext}(s, \mathbf{u}, s'-s)$, $P_{a\,\nu}(s, \mathbf{u}, s'-s)$ or $P_{sc\,\nu}(s, \mathbf{u}, s'-s)$ and $p_\nu(\mathbf{u_1}, \mathbf{u})$ determined as previously. The Beerian semi transparent real phase is characterized by uniform extinction, absorption or scattering coefficients, $\beta_{2\,\nu}$, $\kappa_{2\,\nu}$ or $\sigma_{2\,\nu}$ respectively, a phase function $p_{2\,\nu}$ and possibly a refractive index $n_{2\,\nu}$. In this singular configuration, the previously homogenized phase and the real one occupy the same physical volume $\Pi \mathrm{d}V$.

The extinction phenomena due to the real and the previously homogenized semi transparent phases are statistically independent: In the homogenized phase the opaque wall elements have the same behavior as particles within a gas. Consequently the transmissivity of a column of the global homogenized medium is the product of the transmissivities associated with the two media. The global cumulative distribution function $G_{ext\,g}(s, \mathbf{u}, s'-s)$ then writes

$$1 - G_{ext\,g}(s, \mathbf{u}, s'-s) \;=\; [1 - G_{ext}\,(s, \mathbf{u}, s'-s)]\exp[-\,\beta_{2\,\nu}\,(s'-s)]. \tag{10}$$

3.2.3 Medium with semi transparent phases (ST2) or one of them transparent (STT)

The general case corresponds to two semi transparent phases(ST2) An important particular case deals with a semi transparent phase and a transparent one (STT). These configurations are

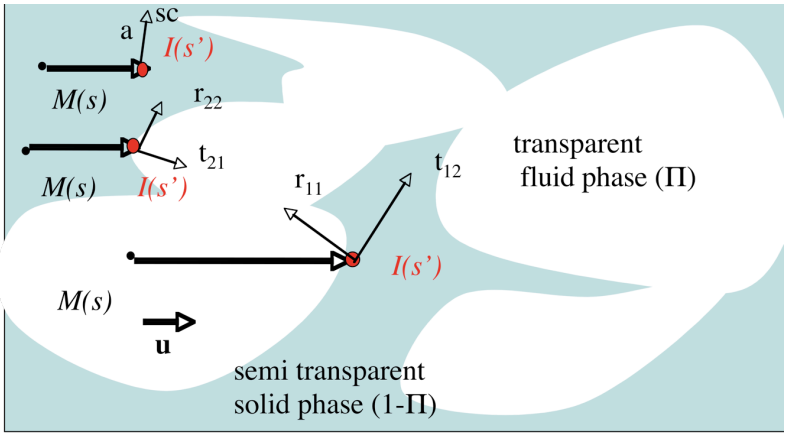

Figure 10: Principles of G_{ext}, P_a, P_{sc} determination (STT case) .

typically encountered when a solid phase is semi transparent at local scale. Additional extinction phenomena occur, as shown in Fig.10, when a ray, issued from any point of this semi transparent phase:

- Hits an interface with the other phase. In the homogenized approach, the ray is then only scattered: This scattering corresponds in the real medium to internal reflection or transmission.

- Is absorbed or scattered within the real semi transparent phase. These phenomena are characterized by an absorption coefficient $\kappa_{\nu\,1}$, a scattering coefficient $\sigma_{\nu\,1}$ and a scattering phase function $p_{\nu\,1}$.

All surface phenomena become volume phenomena within the homogenized propagation phase. Consequently, four scattering phenomena occur, after homogenization, within the semi

transparent phase 1. All of them are characterized by partial cumulative scattering probabilities and phase functions:

- $P_{sc\nu 11}$ and $p_{\nu 11}$ associated with internal reflection (extinction and source terms);
- $P_{sc\nu 12}$ and $p_{\nu 12}$ associated with transmission from 1 to 2 (extinction term);
- $P_{sc\nu 1}$ associated with Beerian scattering within the real medium, characterized by the scattering coefficient $\sigma_{\nu 1}$ and the corresponding phase function $p_{\nu 1}$.
- $P_{sc,\nu 21}$ and $p_{\nu 21}$ associated with transmission from 2 to 1 (source term).

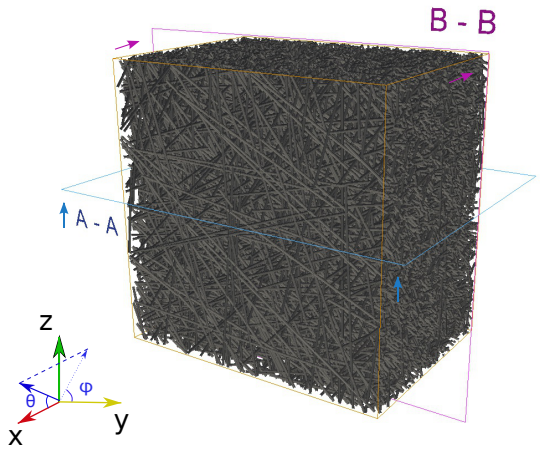

Figure 11: Model of insulation material[23] .

All these scattering phenomena and absorption occur at any point of the homogenized phase: Indeed the presence of both the semi transparent phase and interface elements is only probabilistic. The extinction cumulative distribution function is then given by

$$G_{\nu ext1} = P_{sc\nu 11} + P_{sc\nu 12} + P_{sc\nu 1} + P_{a\nu 1} \tag{11}$$

A homogenized transparent phase 1 is only characterized by $P_{sc\nu 11}$, $P_{sc\nu 12}$, and $P_{sc\nu 21}$ and the associated phase functions.

a) Geometrically defined media

Dauvois[23] has studied an insulation material, shown in Fig.11, which is a set of partially overlapping finite cylinders characterized by two angles: θ with the system axis x and φ azimuth by reference to the x axis. The centers of the cylinders and the φ values are randomly distributed; θ follows a Gaussian distribution: 95% of the angles belong to the range $[0 - 10°]$. These semi transparent cylinders (medium 1), characterized[2] by β, κ, σ and a refractive index n, are immersed in air (medium 2).

The extinction cumulative distribution function within air (interstices) is rigorously Beerian, as previously for DOOS; On the contrary, the extinction cumulative distribution function within the cylinders is strongly non Beerian, as shown in Fig.12.

Four phase functions p_{sc11}, p_{sc12}, p_{sc21} and p_{sc22} are associated with four scattering cumulative probabilities P_{sc11}, P_{sc12}, P_{sc21} and P_{sc22}: They correspond to reflection within cylinders, transmission from cylinders to air, transmission from air to cylinders, reflection within air, respectively. Examples are plotted in Fig.13.

[2]In the case of the work of Dauvois, the medium 1 is only absorbing. Nevertheless, an absorbing and scattering medium 1, more general case, is considered here.

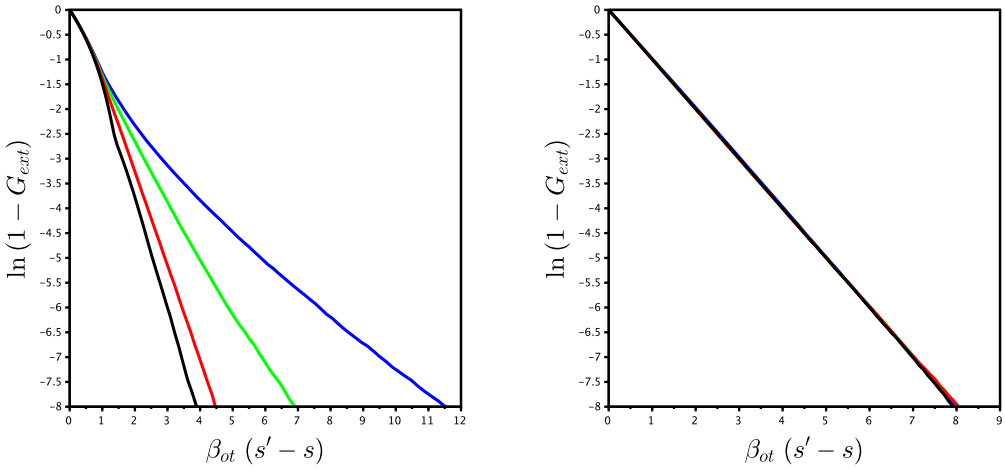

Figure 12: Extinction cumulative distribution functions $G_{ext\,1}(\theta)$ (left) and $G_{ext\,2}(\theta)$ (right) averaged on φ associated with the insulation material[23]. .

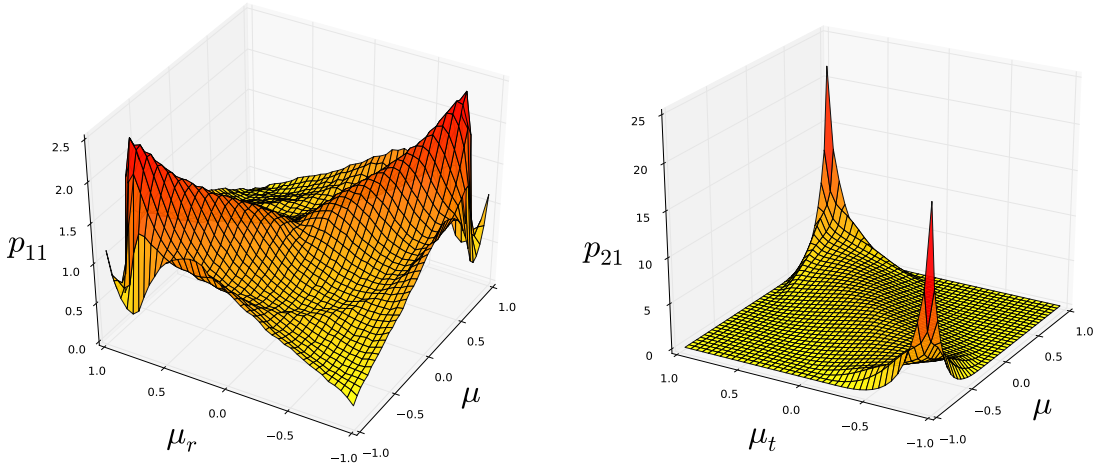

Figure 13: Scattering phase functions p_{11} and p_{21} of the insulation material[23], averaged on azimuth; $\mu = \mathbf{x}.\mathbf{u}_1$, $\mu_r = \mathbf{x}.\mathbf{u}$ (reflection case), $\mu_t = \mathbf{x}.\mathbf{u}$ (transmission case); $\mathbf{u}_1$ and $\mathbf{u}$ incidence and scattering direction unit vectors.

b) Media defined by tomography

Zeghondy et al.[15] have studied both theoretically and experimentally a semi transparent

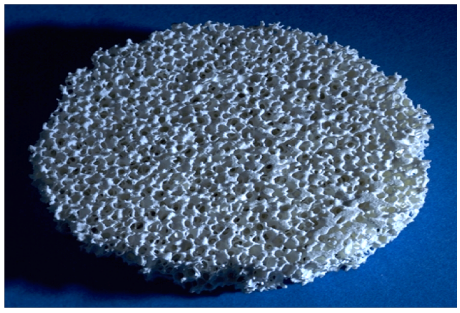

Figure 14: Studied sample of mullite foam[15]; $\Pi = 0.85$.

mullite foam, in the visible range, from X tomography data collected at ESRF(Grenoble). The spatial resolution of the tomography is about $3\,\mu$m. Three representative samples within the tomographied piece, of iteratively defined volume, have been used for checking the homogeneity of the medium. The dispersion of the corresponding results is negligible.

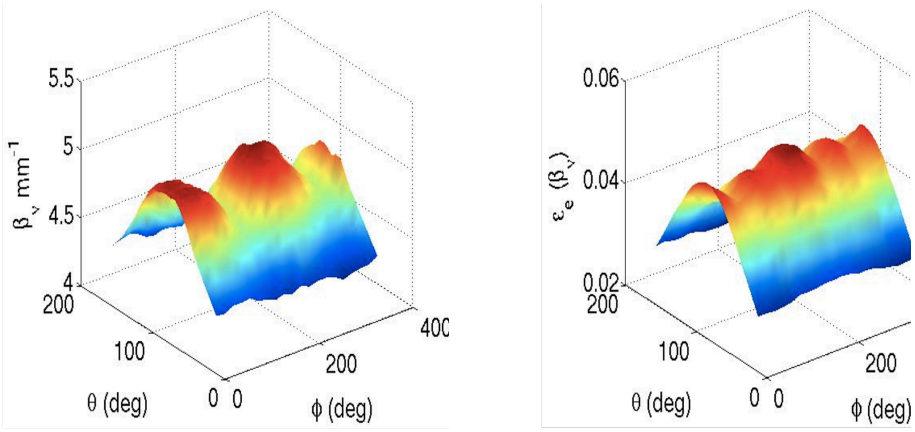

Figure 15: RDFI optimized values of the directional extinction coefficient and RDFI relative standard deviations for a mullite foam[15]; $\Pi = 0.85$.

The directional extinction cumulative distribution function, the absorption cumulative probability and a phase function depending both on the incidence and scattering directions have been determined directly from the radiative properties of the real semi transparent medium and from the Fresnel's laws. G_{ext} and P_a are practically isotropic and Beerian. The phase function depends only on the scattering angle cosine. Optimal RDFI values of the extinction and absorption coefficients β_ν and κ_ν are plotted in Figs.15 and 16 with the associated identification errors, as defined in Sec.2.1.2.

3.3 Statistically non homogeneous media

Zarrouati[11] has studied the radiative properties of a bed of non overlapping opaque spheres at the vicinity of a wall for a medium enclosed between two infinite vertical walls or within an infinite

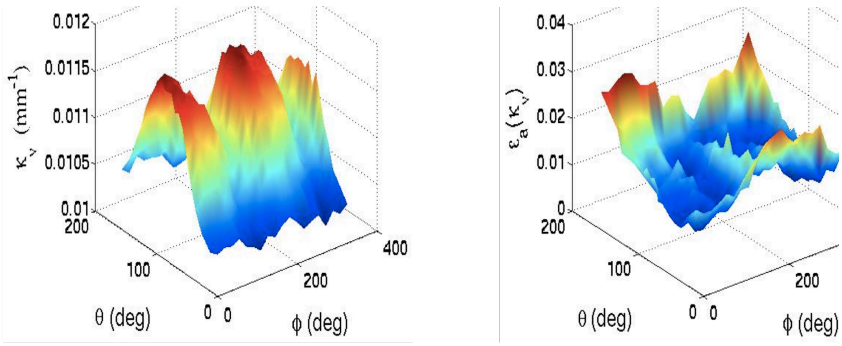

Figure 16: RDFI optimized values of the directional absorption coefficient and relative RDFI standard deviations for a mullite foam[15]; $\Pi = 0.85$.

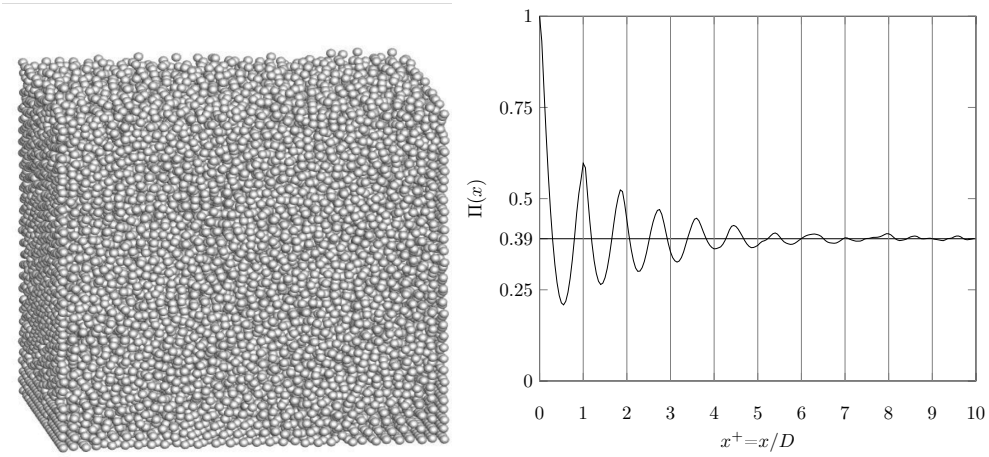

Figure 17: Left: Example of realization of a packed bed of spheres[26, 11]; Right: Porosity field along the direction normal to the wall[11].

cylinder. This study has also been generalized to a bed of opaque finite cylinders enclosed in an infinite cylinder. All these configurations present some statistical symmetries: The resolution is one-dimensional. The morphological data have been obtained from the Digipac^{TM}[26] simulation software. An example of realization is shown in Fig.17 with the corresponding porosity field: Strong variations of the porosity Π occur in the vicinity of a wall. A correct modeling of this strong non homogeneity is important as, in the associated application (fuel reforming), the flux is precisely imposed at the wall by combustion.

Examples of extinction cumulative distribution functions $G_{ext}(s, \mu, s' - s)$ for the plane configuration, are given in Fig.18, where μ is the cosine of the angle between a direction and the axis x normal to the plane walls. If the medium is Beerian far from the walls, it is less and less Beerian when the distance to a wall decreases.

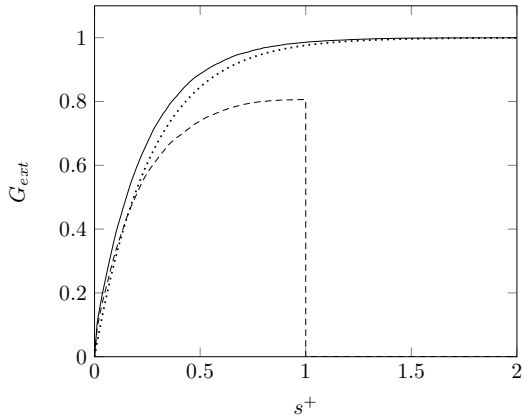

Figure 18: Extinction cumulative distribution function $G_{ext}(x, \mu, s)$ of the packed bed: $x/D = 0.5$; $s^+ = s/D$; $\mu = -0.5$ (dashed curve); $\mu = 0$ (solid curve); Beerian extinction cumulative distribution function characterized by $\beta = \frac{A(x)}{4\Pi(x)}$ (dotted curve).

Regular and periodical systems can also be accurately modeled by extinction cumulative distribution functions $G_{ext}(x, \mu, x' - x)$. Consider, for instance, a square regular rod bundle enclosed between two parallel walls, which are also parallel to the rod axes, on which uniform thermal conditions are imposed. The porosity field is a continuous function along an axis x normal to the walls, which is equal to 1 within the alleys between the rods of axes belonging to the same plane. An approach similar to the previous one can easily be developed in this case, which corresponds to the example of Sec.2.3.1 a) of the companion paper[21].

4 Ideal Thermal Equilibrium and Local Thermal Equilibrium of Radiation

At this step emission has not been modeled. Indeed, it strongly depends on the thermal conditions of the matter and is studied in the companion paper[21]. As in the classical theory of radiation, emission is defined by reference to Ideal Thermal Equilibrium (ITE) conditions. The study of a medium in these conditions, developed in Sec.4.1.1, is then essential. In particular, generalized extinction, absorption and scattering coefficients can be introduced at equilibrium far from the porous medium boundaries.

On the other hand, radiation is generally considered in ballistic regime in open fields. But, in many applications, a porous medium is practically isothermal along some extinction lengths,

typically some pore sizes. The radiation field is then practically at Local Thermal Equilibrium (LTE): An optically thick cell of the medium is practically at equilibrium and the radiative transfer can simply be considered as a small perturbation of these LTE conditions. In this important particular case, the GRTE degenerates into a simple RTE, introduced in Sec.4.2. Moreover, some key properties of the phase functions and the scattering coefficients introduced at LTE are also presented in Sec.4.3.

This Section is limited to statistically homogeneous phases, possibly strongly anisotropic and non Beerian. Statistically non homogeneous media are studied in the companion paper[21].

4.1 Ideal Thermal Equilibrium of Radiation

4.1.1 Generalized extinction, absorption and scattering coefficients at equilibrium far from the boundaries

In ideal thermal equilibrium conditions, the intensity associated with a homogenized phase, of fraction per unit volume Π, is $\Pi\, n_\nu^2(\mathbf{u})\, I_\nu^\circ(T)$, where $n_\nu(\mathbf{u})$ is the phase refractive index. The total source term $S_\nu^\circ(\mathbf{u})$, sum of the emission and scattering source terms, is spatially uniform, only if the distance to any boundary $s' - s_b$ corresponds to an optically thick medium, *i.e.* if $S_\nu^\circ(\mathbf{u})$ at the point s' is independent of the boundary condition in s_b. Equation 4 then becomes in ideal equilibrium conditions (see also Fig.1)

$$\Pi\, n_\nu^2(\mathbf{u})\, I_\nu^\circ(T) \;=\; S_\nu^\circ(\mathbf{u},\, T) \int_{-\infty}^{s'} [1 \;-\; G_{ext\,\nu}(\mathbf{u}, s' - s)]\, \mathrm{d}s. \tag{12}$$

The total source term $S_\nu^\circ(\mathbf{u},\, T)$ is, in these conditions, equal to the extinction term and also writes

$$S_\nu^\circ(\mathbf{u},\, T) \;=\; B_\nu(\mathbf{u})\, \Pi\, n_\nu^2\,(\mathbf{u})\, I_\nu^\circ(T), \tag{13}$$

equation which defines the *generalized extinction coefficient at equilibrium* $B_\nu(\mathbf{u})$, far from the porous medium boundaries

$$B_\nu(\mathbf{u}) \;=\; \frac{1}{\int_0^\infty [1 \;-\; G_{ext\,\nu}(\mathbf{u}, v)]\, \mathrm{d}v}. \tag{14}$$

It is easy to verify that, in the case of a Beerian medium characterized by the extinction coefficient $\beta_\nu(\mathbf{u})$, $B_\nu(\mathbf{u})$ is equal to $\beta_\nu(\mathbf{u})$. $B_\nu(\mathbf{u})$ represents the extinction between s' and $s' + \mathrm{d}s'$ of all contributions to the intensity $\Pi\, n_\nu^2\,(\mathbf{u})\, I_\nu^\circ(T)$ in s' due to all the source terms from infinity to s' in the direction $\mathbf{u}$.

The flux per unit volume and unit solid angle associated with all these source terms and extinguished between s' and $s' + \mathrm{d}s'$ by any type of scattering (i, ii or iii), defined in Sec.2.2, simply becomes

$$\int_{-\infty}^{s'} \frac{\mathrm{d}P_{sc\,\nu}(\mathbf{u}, s' - s)}{\mathrm{d}s'}\, B_\nu(\mathbf{u})\, \Pi\, n_\nu^2\,(\mathbf{u})\, I_\nu^\circ(T)\, \mathrm{d}s \;=\; P_{sc\,\nu}(\mathbf{u}, \infty)\, B_\nu(\mathbf{u})\, \Pi\, n_\nu^2\,(\mathbf{u})\, I_\nu^\circ(T), \tag{15}$$

where $P_{sc\,\nu}(\mathbf{u}, \infty)$, is the albedo of the homogenized phase for this type of scattering and the direction $\mathbf{u}$.

If we consider, for the sake of simplicity, the case of a porous medium with a transparent phase and an opaque one (OT), characterized by a unique type ii) of scattering, the *generalized scattering coefficient at equilibrium* $\Sigma_\nu(\mathbf{u})$ and, correlatively, the *generalized absorption coefficient at equilibrium* $K_\nu(\mathbf{u})$ are defined by

$$\Sigma_\nu(\mathbf{u}) \;=\; P_{sc\,\nu}(\mathbf{u}, \infty)\, B_\nu(\mathbf{u}), \qquad K_\nu(\mathbf{u}) \;=\; B_\nu(\mathbf{u}) \;-\; \Sigma_\nu(\mathbf{u}) \;=\; [1 - P_{sc\,\nu}(\mathbf{u}, \infty)]\, B_\nu(\mathbf{u}). \tag{16}$$

Note that, in the common case of a porous medium with a transparent phase and an opaque one, characterized by a diffuse and gray absorptivity α, the albedo $P_{sc}(\mathbf{u}, \infty)$ is equal to $1 - \alpha$. Consequently: $K_\nu(\mathbf{u}) = \alpha\, B_\nu(\mathbf{u})$, $\Sigma_\nu(\mathbf{u}) = (1 - \alpha)\, B_\nu(\mathbf{u})$.

4.1.2 Behavior of G_{ext} at the optically thick limit

The properties of the extinction cumulative distribution functions at the optically thick limit are linked to the generalized extinction coefficient at equilibrium. It has been observed in Sec.3

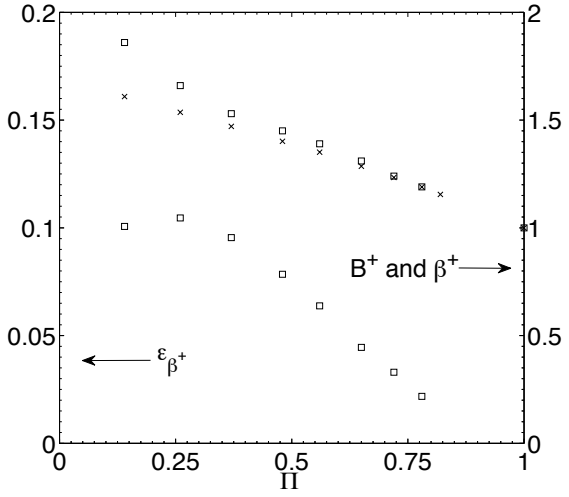

Figure 19: β^+ (squares)and B^+ (crosses) normalized values β_{RDFI}/β_{OT} and B/β_{OT} of the RDFI extinction coefficient and generalized extinction coefficient at equilibrium for DOTS[20]; RDFI relative standard deviations associated with β^+; $\beta_{OT} = A/(4\Pi)$.

that, for non Beerian media, the slope of the logarithm of the transmissivity $1 - G_{ext}(\mathbf{u}, s' - s)$:

- Is equal to the opposite of β_{OT}, extinction coefficient at the optically thin limit, for very small $s' - s$ values: $\beta_{OT}(s' - s) << 1$;

- Strongly varies in the intermediate optical thickness range ;

- Finally tends to the uniform value $-B(\mathbf{u})$ at the optically thick limit characterized by $\beta_{OT}(s' - s) >> 1$ (see, for instance Figs.4 and 12). Indeed, in these particular conditions, the generalized extinction coefficient at equilibrium $B(\mathbf{u})$ can be defined. This important property allows, under precise conditions, a radiative Fourier's law to be introduced, as shown in the companion paper[21].

Note that, in the commonly encountered case of a medium which is not rigorously but approximately Beerian, β_{OT}, B and the optimized extinction coefficient obtained by the RDFI method β_{RDFI} take different values, as shown in Fig.19 dedicated to the DOTS, introduced in Sec.3.2.1.

4.2 Local Thermal Equilibrium of Radiation

A cell of the system is at Local Thermal Equilibrium of Radiation if:

- i) Along a distance δ over which it is optically thick it is practically isothermal. A precise quantitative condition is given in Sec.1.1 of the companion paper[21];

- ii) Its distance to any boundary of the porous medium also corresponds to an optically thick medium: The cell is not directly influenced by the thermal conditions at the boundaries.

Under these conditions, the cell can be characterized by a temperature $T(\mathbf{X})$ and the variations of this temperature only occur at a macro scale $\mathbf{X}$ larger than δ. But a radiative flux appears at the scale $\mathbf{X}$, as a small perturbation of its LTE conditions.

It has been shown[20] that, at LTE conditions, the GRTE degenerates into a RTE,, characterized by the generalized extinction, absorption and scattering coefficients at equilibrium of Sec.4.1.1. In the OT case, this RTE writes, for a statistically homogeneous but anisotropic homogenized phase associated with interface elements

$$\begin{aligned} \Pi \frac{\mathrm{d}I_\nu}{\mathrm{d}s}(\mathbf{u},\mathbf{X}) &+ \Pi\, B_i(\mathbf{u})\, I_\nu(\mathbf{u},\mathbf{X}) \\ &= \Pi\, K_{\nu\, i}(\mathbf{u}) n_\nu^2\, I_\nu^\circ[T_i(\mathbf{X})] + \Pi \frac{1}{4\pi} \int_{4\pi} \Sigma_{\nu\, i}(\mathbf{u}_1) p_{\nu\, i}(\mathbf{u}_1,\mathbf{u}) I_\nu(\mathbf{u}_1,\mathbf{X}) \mathrm{d}\Omega_1. \quad (17) \end{aligned}$$

In practice, Equation 17 is not solved by classical radiative transfer methods, but only solved by a perturbation technique which leads to a radiative tensor, associated to a radiative Fourier's law. This method is developed in the companion paper[21]. Nevertheless, in some cases in which condition ii) is fulfilled, but not condition i), this RTE has to be directly solved.

4.3 Some scattering properties at LTE (homogeneous phases)

The conditions of Local Thermal Equilibrium of the radiation field and the associated RTE, defined in the previous Section, are assumed fulfilled. In these conditions, some key properties of scattering, associated with both reflection (all cases) and transmission (STT ad ST2 cases), are introduced in the present Section.

4.3.1 Scattering associated with reflection (all cases)

In the OT, OST, STT and ST2 models based on radiative statistical distribution functions, two media coexist within the same physical volume $\Pi\, \mathrm{d}V$ statistically devoted to the fluid phase:

- the propagation phase characterized by a refractive index n_ν which is transparent (OT, STT) or semi transparent (OST, STT and ST2) and, in these last cases, also characterized by absorption, scattering and extinction coefficients,

- an effective semi transparent medium i associated with a statistical distribution of interface elements. The first developments of the statistical homogenization have been founded on an interfacial effective refractive index $n_{\nu\, i}(\mathbf{u})$[12, 13, 22], what will also be done in Sec.4.3.3, but it is simpler to base the model on the real transparent or semi transparent medium, which is done in the present Section and the following one.

The scattering source term per unit volume and unit solid angle $\mathrm{d}\Omega(\mathbf{u})$ associated with interfacial reflection writes

$$S_{sc}(\mathbf{u}) = \int_{4\pi} \Pi\, \Sigma_\nu(\mathbf{u_1})\, \frac{p_\nu(\mathbf{u}_1,\mathbf{u})}{4\pi}\, I_\nu(\mathbf{u}_1)\, \mathrm{d}\Omega(\mathbf{u}_1). \quad (18)$$

The application of the general reciprocity theorem to the scattering of an elementary beam $\mathrm{d}\Omega_1$ within the homogenized semi transparent medium, expressed in this medium, in ITE conditions, leads to

$$\begin{aligned} &\Sigma_\nu(\mathbf{u}_1)\, \Pi\, n_\nu^2\, I_\nu^\circ(T)\, \mathrm{d}\Omega(\mathbf{u}_1) \left[\frac{p_\nu\,(\mathbf{u}_1,\mathbf{u})}{4\pi}\, \mathrm{d}\Omega(\mathbf{u})\right] \\ = \;& \Sigma_\nu(-\mathbf{u})\, \Pi\, n_\nu^2\, I_\nu^\circ(T)\, \mathrm{d}\Omega(-\mathbf{u}) \left[\frac{p_\nu(-\mathbf{u},-\mathbf{u}_1)}{4\pi}\, \mathrm{d}\Omega(-\mathbf{u}_1)\right]. \quad (19) \end{aligned}$$

$$i.e. \qquad \Sigma_\nu(\mathbf{u}_1)\, p_\nu(\mathbf{u}_1, \mathbf{u}) \;=\; \Sigma_\nu(-\mathbf{u})\, p_\nu(-\mathbf{u}, -\mathbf{u}_1) \tag{20}$$

The scattering source term per unit volume and unit solid angle $\mathrm{d}\Omega(\mathbf{u})$ given by Eq.18 then becomes

$$S_{sc}(\mathbf{u}) \;=\; \Pi\, \Sigma_\nu(-\mathbf{u}) \int_{4\pi} \frac{p_\nu(-\mathbf{u}, -\mathbf{u}_1)}{4\pi}\, I_\nu(\mathbf{u}_1)\, \mathrm{d}\Omega(\mathbf{u}_1). \tag{21}$$

In ITE conditions, this term is equal to $\Pi\, \Sigma_\nu(-\mathbf{u})\, n_\nu^2\, I_\nu^\circ(T)$. It is also equal to the extinction term by scattering in the direction $\mathbf{u}$, *i.e* $\Pi\, \Sigma_\nu(\mathbf{u})\, n_\nu^2\, I_\nu^\circ(T)$. Consequently

$$\Sigma_\nu(-\mathbf{u}) \;=\; \Sigma_\nu(\mathbf{u}), \tag{22}$$

and finally the scattering source term per unit volume and unit solid angle $\mathrm{d}\Omega(\mathbf{u})$, expressed in the real medium simply writes

$$S_{sc}(\mathbf{u}) \;=\; \Pi\, \Sigma_\nu(\mathbf{u}) \int_{4\pi} \frac{p_\nu(-\mathbf{u}, -\mathbf{u}_1)}{4\pi}\, I_\nu(\mathbf{u}_1)\, \mathrm{d}\Omega(\mathbf{u}_1), \tag{23}$$

Note that $p_{\nu\,12}(-\mathbf{u}_1, -\mathbf{u}_2)$, which is rigorously equal[27] to $p_{\nu\,12}(-\mathbf{u}_2, -\mathbf{u}_1)$, is also commonly equal to $p_{\nu\,12}(\mathbf{u}_1, \mathbf{u}_2)$, due to the system macroscopic statistical symmetries.

4.3.2 Scattering associated with transmission (STT and ST2)

In the following, the intensity within a medium j expressed in a medium k of refractive index $n_{\nu\,k}$ is noted $I_{\nu\,jk}$. The elementary solid angles $\mathrm{d}\Omega_1$, $\mathrm{d}\Omega_2$ and $\mathrm{d}\Omega_v$ are associated with the media 1, 2 and the void of refractive indices $n_{\nu\,1}$, $n_{\nu\,2}$ and 1 respectively.

Consider a transmission from a medium 2 of refractive index $n_{\nu\,2}$ to a medium 1 of refractive index $n_{\nu\,1}$. The phase function which is called $p_{\nu\,21}$ now associates a scattered intensity within medium 1 with an incident flux per unit volume within medium 2. Precise definitions of the bidirectional transmissivity and of the phase function associated with scattering by transmission between phases are given in Appendices A and B. $S_{sc\,\nu\,21}$, the corresponding scattering source term per unit volume and unit solid angle $\mathrm{d}\Omega_1(\mathbf{u}_1)$ then writes

$$S_{sc\,\nu\,21}(\mathbf{u}_1) \;=\; \int_{4\pi} \Sigma_{\nu\,21}(\mathbf{u_2})\, \frac{p_{\nu\,21}(\mathbf{u}_2, \mathbf{u}_1)}{4\pi}\, \Pi_2\, I_{\nu\,22}(\mathbf{u}_2)\, \mathrm{d}\Omega_2(\mathbf{u_2}). \tag{24}$$

The refractive indices are linked to the elementary solid angles in the media 1 , 2 and the void v by

$$n_{\nu\,1}^2\, \mathrm{d}\Omega_1 \;=\; n_{\nu\,2}^2\, \mathrm{d}\Omega_2 \;= \mathrm{d}\Omega_v. \tag{25}$$

and similarly, from the Clausius theorem, the intensities within a medium j expressed in media 1, 2 and v are linked by

$$I_{\nu\,j1}\, \mathrm{d}\Omega_1 \;=\; I_{\nu\,j2}\, \mathrm{d}\Omega_2 \;=\; I_{\nu\,jv}\, \mathrm{d}\Omega_v. \tag{26}$$

The general reciprocity theorem applied to scattering by transmission (incident elementary beam $\mathrm{d}\Omega_1$, scattered elementary beam $\mathrm{d}\Omega_2$), in ITE conditions, expressed in void, then leads to

$$\begin{aligned} & \Sigma_{\nu\,21}(\mathbf{u}_2)\, \Pi_2\, I_\nu^\circ(T) \mathrm{d}\Omega_v(\mathbf{u}_2)\, [\frac{p_{\nu\,21}(\mathbf{u}_2, \mathbf{u}_1)}{4\pi}\, \frac{\mathrm{d}\Omega_v(\mathbf{u}_1)}{n_{\nu\,1}^2})] \\ = \;& \Sigma_{\nu\,12}(-\mathbf{u}_1)\, \Pi_1\, I_\nu^\circ(T) \mathrm{d}\Omega_v(-\mathbf{u}_1)\, [\frac{p_{\nu\,12}(-\mathbf{u}_1, -\mathbf{u}_2)}{4\pi}\, \frac{\mathrm{d}\Omega_v(-\mathbf{u}_2)}{n_{\nu\,2}^2}], \end{aligned} \tag{27}$$

or

$$\Sigma_{\nu\,21}(\mathbf{u}_2)\, \Pi_2\, n_{\nu\,2}^2\, p_{\nu\,21}(\mathbf{u}_2, \mathbf{u}_1) \;=\; \Sigma_{\nu\,12}(-\mathbf{u}_1)\, \Pi_1\, n_{\nu\,1}^2\, p_{\nu\,12}(-\mathbf{u}_1, -\mathbf{u}_2) \tag{28}$$

and Equation 24 becomes

$$S_{sc\,\nu\,21}(\mathbf{u}_1) \;=\; \Sigma_{\nu\,12}(-\mathbf{u}_1)\,\Pi_1 \int_{4\pi} \frac{p_{\nu\,12}(-\mathbf{u}_1,-\mathbf{u}_2)}{4\pi}\,(\frac{n^2_{\nu\,1}}{n^2_{\nu\,2}})\,I_{\nu\,22}(\mathbf{u}_2)\,\mathrm{d}\Omega_2(\mathbf{u_2}). \tag{29}$$

In ITE conditions, this quantity is equal to $\Sigma_{\nu\,12}(-\mathbf{u_1})\,\Pi_1\,n^2_{\nu\,1}\,I^\circ_\nu(T)$, and is also equal to the scattering extinction term in medium 1 associated with transmission to medium 2, *i.e.* $\Sigma_{\nu\,12}(\mathbf{u_1})\,\Pi_1\,n^2_{\nu\,1}\,I^\circ_\nu(T)$. Consequently

$$\Sigma_{\nu\,12}(-\mathbf{u}_1) \;=\; \Sigma_{\nu\,12}(\mathbf{u}_1), \tag{30}$$

and finally the scattering source term per unit volume and unit solid angle $\mathrm{d}\Omega_1(\mathbf{u}_1)$ also writes in terms of quantities related to media 1 and 2

$$S_{sc\,\nu\,21}(\mathbf{u}_1) \;\;=\;\; \Pi_1\,(\frac{n^2_{\nu\,1}}{n^2_{\nu\,2}})\Sigma_{\nu\,12}(\mathbf{u}_1) \int_{4\pi} \frac{p_{\nu\,12}(-\mathbf{u}_1,-\mathbf{u}_2)}{4\pi}\;I_{\nu\,22}\,\mathrm{d}\Omega_2(\mathbf{u}_2). \tag{31}$$

The factor $n^2_{\nu\,1}/n^2_{\nu\,2}$ results from the definition of a phase function from a medium 2 to a medium 1, which is expressed in medium 1. As, by reciprocity, the source term by scattering from 2 to 1 has been expressed vs the phase function from 1 to 2, the factor $n^2_{\nu\,1}/n^2_{\nu\,2}$ allows the result to be expressed in medium 1.

The phase function $p_{\nu\,12}(-\mathbf{u}_1,-\mathbf{u}_2)$, which is rigorously equal[27] to $p_{\nu\,12}(-\mathbf{u}_2,-\mathbf{u}_1)$, is also commonly equal to $p_{\nu\,12}(\mathbf{u}_1,\mathbf{u}_2)$ due to system macroscopic statistical symmetries.

4.3.3 Scattering model based on an effective refractive index

This model will only be introduced in the case of scattering associated with reflection. The results of Sec.4.3.1 can also be obtained by considering the effective semi transparent medium i associated with the statistical distribution of interface elements within $\Pi \mathrm{d}V$. This medium is characterized by the radiative coefficients $B_\nu(\mathbf{u})$, $K_\nu(\mathbf{u})$, $\Sigma_\nu(\mathbf{u})$ and the phase function $p_\nu(\mathbf{u}_1,\mathbf{u})$, and also an effective refractive index $n_{\nu\,i}(\mathbf{u})$.

Note that, according to the Clausius theorem, the elementary solid angle becomes $\mathrm{d}\Omega_i$ in the virtual homogenized phase. It is linked to the elementary solid angle $\mathrm{d}\Omega$ in the real propagation medium of refractive index n_ν and to the solid angle $\mathrm{d}\Omega_v$ in the void by

$$\mathrm{d}\Omega_i(\mathbf{u})\,n^2_{\nu\,i}(\mathbf{u}) \;=\; \mathrm{d}\Omega(\mathbf{u})\,n^2_\nu \;=\; \mathrm{d}\Omega_v(\mathbf{u}). \tag{32}$$

In ITE conditions, $S^\circ_{\nu\,sc}(\mathbf{u})$, the scattering source term per unit volume and unit solid angle $\mathrm{d}\Omega_i(\mathbf{u})$, associated with reflection on interfaces in the real medium, writes

$$S^\circ_{\nu\,sc}(\mathbf{u}) \;=\; \int_{4\pi} \Pi\,\Sigma_{\nu\,i}(\mathbf{u_1})\;\frac{p_\nu(\mathbf{u}_1,\mathbf{u})}{4\pi}\;n^2_{\nu\,i}(\mathbf{u_1})\,I^\circ_\nu(T)\,\mathrm{d}\Omega_i(\mathbf{u}_1). \tag{33}$$

This quantity is equal to the term of extinction by scattering in ITE conditions, *i.e.*

$$S^\circ_{\nu\,ext_{sc}}(\mathbf{u}) \;=\; \Sigma_{\nu\,i}(\mathbf{u})\,\Pi\,n^2_{\nu\,i}(\mathbf{u})\,I^\circ_\nu(T). \tag{34}$$

In these conditions, the unique solution verifies

$$\Sigma_{\nu\,i}(\mathbf{u})\,n^2_{\nu\,i}(\mathbf{u}) \;=\; C_\nu. \tag{35}$$

As this product is independent of $\mathbf{u}$, $S_{\nu\,sc}$, the scattering source term per unit volume writes

$$S_{\nu\,sc}(\mathbf{u})\,\mathrm{d}\Omega_i(\mathbf{u}) \;=\; \Pi\,\mathrm{d}\Omega_i(\mathbf{u})\,\Sigma_{\nu\,i}(\mathbf{u})\;n^2_{\nu\,i}(\mathbf{u}) \int_{4\pi} \frac{p_\nu(\mathbf{u}_1,\mathbf{u})}{4\pi}\;I_{\nu\,v}(\mathbf{u}_1)\,\mathrm{d}\Omega_i(\mathbf{u}_1). \tag{36}$$

where $I_{\nu\, v}$ is the intensity in the void, of refractive index equal to 1. By using the Clausius theorem, Equation 36 becomes

$$S_{\nu\, sc}(\mathbf{u})\, \mathrm{d}\Omega(\mathbf{u}) \;=\; \Pi\, \mathrm{d}\Omega(\mathbf{u})\, \Sigma_\nu(\mathbf{u}) \int_{4\pi} \frac{p_\nu(\mathbf{u}_1, \mathbf{u})}{4\pi}\, I_\nu(\mathbf{u}_1)\, \mathrm{d}\Omega(\mathbf{u}_1). \tag{37}$$

where I_ν equal to $n_\nu^2\, I_{\nu\, v}$ is the intensity in the real propagation phase. The results are identical to those of Sec.4.3.1.

5 Conclusion

Scattering, absorption and extinction properties of porous media with opaque and transparent phases (OT), opaque and semi transparent phases (OST), semi transparent phases (ST2), semi transparent and transparent phases (SST) have been exhaustively characterized by radiative statistical distribution functions and a general scattering phase function depending on both incidence and scattering directions. This model also allows homogenized phases of a porous medium, which do not follow the Beer's extinction law, to be accurately characterized: It is the case of most of the interfacial scattering and absorption phenomena for OT, OST, ST2 and STT configurations. In this case, extinction, absorption and scattering coefficients have no physical meaning. Indeed, they can only be defined for Beerian homogenized phases. The validity of Beer's law can be accurately verified by the RDFI method.

Emission is studied in the companion paper[21]. Indeed, this phenomenon depends both on the matter radiative properties and the temperature field within the system. Consequently, emission modeling depends on the thermal conditions of the homogenized phase. When a Beerian absorption coefficient κ_ν can be defined, the emission source term is simply $\kappa_\nu\, n_\nu^2\, I_\nu^\circ(T)$. This model is always valid for ST2 and STT configurations. But, emission by non Beerian interfacial opaque elements, often encountered in OT and OST configurations, can only be expressed from the reciprocity theorem applied to the GRTE: This approach is developed in the companion paper[21], more generally dedicated to radiative transfer.

A Appendix: Bidirectional reflectivity and transmissivity

Theoretically, the reflection and transmission laws at local scale are characterized by bidirectional reflectivity and transmissivity $\rho''_\nu(\mathbf{u}_i, \mathbf{u}_r)$ and $\tau''_\nu(\mathbf{u}_i, \mathbf{u}_t)$. These real quantities are generally unknown: Their determination is difficult. From a practical point of view, opaque interfaces are generally characterized by a diffuse reflection law, a specular one or a linear combination of these laws. Interfaces between semi transparent or transparent phases are generally characterized by Fresnel laws. All these models are characterized by the corresponding $\rho''_\nu(\mathbf{u}_i, \mathbf{u}_r)$ or $\tau''_\nu(\mathbf{u}_i, \mathbf{u}_t)$ expressions.

$\rho''_\nu(\mathbf{u}_i, \mathbf{u}_r)$ or $\tau''_\nu(\mathbf{u}_i, \mathbf{u}_t)$ are defined *in the local frame built around the unit vector normal to an interface* and have precise definitions:

$$\begin{aligned}
\rho''_\nu(\mathbf{u}_i, \mathbf{u}_r) &= \frac{I^r_\nu(\mathbf{u}_r)}{\mathrm{d}\Phi^i_\nu(\mathbf{u}_i)} = \frac{I^r_\nu(\mathbf{u}_r)}{I^i_\nu(\mathbf{u}_i)\cos(\theta_i)\mathrm{d}\Omega_i(\mathbf{u}_i)} \\
\tau''_\nu(\mathbf{u}_i, \mathbf{u}_t) &= \frac{I^t_\nu(\mathbf{u}_t)}{\mathrm{d}\Phi^i_\nu(\mathbf{u}_i)} = \frac{I^t_\nu(\mathbf{u}_t)}{I^i_\nu(\mathbf{u}_i)\cos(\theta_i)\mathrm{d}\Omega_i(\mathbf{u}_i)}
\end{aligned} \tag{38}$$

where I^i_ν, I^r_ν and I^t_ν are the incident, reflected and transmitted intensities, $\mathrm{d}\Phi^i_\nu(\mathbf{u}_i)$ the incident flux and $\mathbf{u}_i$, $\mathbf{u}_r$ and $\mathbf{u}_t$ are the incidence, reflection and transmission direction unit vectors;

$\cos(\theta_i)$ is equal to $\mathbf{n}.\mathbf{u}_i$, where $\mathbf{n}$ is the normal unit vector to the considered surface element. Note that the expression of the incident flux is independent of the medium in which it is expressed. The bidirectional reflectivity or transmissivity then depends on the refractive index of the reflection or transmission medium.

By convention, I_ν^r and I_ν^t, and consequently $\rho''_\nu(\mathbf{u}_r)$ and $\tau''_\nu(\mathbf{u}_t)$ are expressed in the reflection or transmission medium, characterized by the refractive index $n_{\nu\, r}$ or $n_{\nu\, t}$.

B Appendix: Scattering phase functions

The phase functions are defined in the frame of the whole porous medium and couple an incidence direction in this frame $\mathbf{u}$ to a scattering direction $\mathbf{u}_{sc}$ of the same frame. The definitions of the scattering phase functions associated with reflection or transmission in the real medium are based on the ones of the associated bidirectional reflectivities and transmissivities, defined at local scale by reference to a unit vector normal to the surface element.

In the case of scattering corresponding to reflection at local scale, a normal unit vector $\mathbf{n}(\mathbf{r},\mathbf{u})$ is associated at any impact point of a ray issued from any point $M(\mathbf{r})$ of the phase (in the case of a statistically homogeneous medium), in any incidence direction $\mathbf{u}$. The quantity $p_\nu(\mathbf{u},\mathbf{u}_{sc})\,\mathrm{d}\Omega(\mathbf{u}_{sc})/(4\pi)$ is the probability that the energy will be scattered in the elementary solid angle $\mathrm{d}\Omega(\mathbf{u}_{sc})$ around the direction $\mathbf{u}_{sc}$, *i.e*

$$p_\nu(\mathbf{u},\mathbf{u}_{sc})\,\frac{\mathrm{d}\Omega(\mathbf{u}_{sc})}{4\pi} = \frac{\mathrm{d}\Omega(\mathbf{u}_{sc}) \quad (\frac{1}{\Pi V})\int_{\Pi V\,/\,-\mathbf{u}_{sc}.\mathbf{n}\geq 0} \rho''_\nu[\mathbf{u},\mathbf{u}_{sc},\mathbf{n}\,(\mathbf{r},\mathbf{u})] \quad (-\mathbf{n}.\mathbf{u})(\mathbf{r},\mathbf{u})\,\mathrm{d}\mathbf{r}}{\int_{4\pi}(\frac{1}{\Pi V})\int_{\Pi V\,/\,-\mathbf{u}_{sc}.\mathbf{n}\geq 0} \rho''_\nu[\mathbf{u},\mathbf{u}_{sc},\mathbf{n}\,(\mathbf{r},\mathbf{u})] \quad (-\mathbf{n}.\mathbf{u})(\mathbf{r},\mathbf{u})\,\mathrm{d}\mathbf{r}\,\mathrm{d}\Omega(\mathbf{u}_{sc})}. \quad (39)$$

Similarly, in the case of scattering corresponding to transmission at local scale, and with the same notations the phase function writes vs the bidirectional transmissivity

$$p_\nu(\mathbf{u},\mathbf{u}_{sc})\,\frac{\mathrm{d}\Omega(\mathbf{u}_{sc})}{4\pi} = \frac{\mathrm{d}\Omega(\mathbf{u}_{sc}) \quad (\frac{1}{\Pi V})\int_{\Pi V\,/\,\mathbf{u}_{sc}\mathbf{n}\geq 0} \tau''_\nu[\mathbf{u},\mathbf{u}_{sc},\mathbf{n}\,(\mathbf{r},\mathbf{u})] \quad (-\mathbf{n}.\mathbf{u})(\mathbf{r},\mathbf{u})\,\mathrm{d}\mathbf{r}}{\int_{4\pi}(\frac{1}{\Pi V})\int_{\Pi V\,/\,\mathbf{u}_{sc}.\mathbf{n}\geq 0} \tau''_\nu[\mathbf{u},\mathbf{u}_{sc},\mathbf{n}\,(\mathbf{r},\mathbf{u})] \quad (-\mathbf{n}.\mathbf{u})(\mathbf{r},\mathbf{u})\,\mathrm{d}\mathbf{r}\,\mathrm{d}\Omega(\mathbf{u}_{sc})}. \quad (40)$$

In practice, a scattered intensity I_ν^{sc} is associated by the phase function $p_\nu(\mathbf{u},\mathbf{u}_{sc})$ with an incident flux per unit volume and frequency $I_\nu\,\mathrm{d}\Omega(\mathbf{u})$, which, due to the Clausius theorem, is a quantity independent of the medium (initial, final or void).

As for bidirectional reflectivity or transmissivity, $p_\nu(\mathbf{u},\mathbf{u}_{sc})$ *is, by convention, expressed in the scattering medium, characterized by the refractive index $n_{\nu\, sc}$, i.e I_ν^{sc}* is expressed in this medium.

Expressions of the phase functions are given in Ref.[27] in the case of diffuse and specular reflection laws.

References

[1] L. G. Henyey and J. L. Greenstein. *Astrophys. J.*, 93:70, 1941.

[2] L. Glicksman, Shuetz, and Sinofsky. Radiation heat transfer in foam insulation. *International Journal of Heat and Mass Transfer*, 1(30):187–197, 1987.

[3] T.J. Hendricks and J.R. Howell. Inverse radiative analysis to determine spectral radiative properties using the discrete ordinates method. *International Journal of Heat and Mass Transfer*, 2:75–80, 1994.

[4] T. J. Hendricks and J. R. Howell. Absorption/scattering coefficients and scattering phase function in reticulated porous ceramics. *ASME Journal of Heat Transfer.*, 118(1):79–87, 1996.

[5] T.J. Hendricks and J.R. Howell. New radiative analysis approach for reticulated porous ceramics using discrete ordinates method. *Journal of Heat Transfer*, 4(118):911–917, 1996.

[6] Y.S. Yang, J.R. Howell, and D.E. Klein. Radiative heat transfer through a randomly packed bed of spheres by the Monte Carlo method. *Journal of Heat Transfer*, 105:325–332, 1983.

[7] D. Doermann and J. F. Sacadura. Heat transfer in open cell foam insulation. *ASME Journal of Heat Transfer*, 118:88–93, 1996.

[8] D. Baillis, M. Raynaud, and J. F. Sacadura. Spectral radiative properties of open-cell foam insulation. *Journal of Thermophysics and Heat Transfer*, 13(3):292–298, 1999.

[9] R. Lopes, M. Luis, D. Baillis, and J. F. Sacadura. Directional spectral emittance of a packed bed: Correlation between theoretical prediction and experimental data. *ASME Journal of Heat Transfer*, 123:240–248, 2001.

[10] D. Baillis and J. F. Sacadura. Thermal radiation properties of dispersed media: theoretical prediction and experimental characterization. *Journal of Quantitative Spectroscopy and Radiative Transfer*, 67(5):327–363, 2000.

[11] M. Zarrouati, F. Enguehard, and J Taine. Radiative transfer within strongly non homogeneous porous media: Application to a slab of packed particles. *International Journal of Heat and Mass Transfer*, 2015 (in press).

[12] F. Bellet, E. Chalopin, F. Fichot, E. Iacona, and J. Taine. RDFI determination of anisotropic and scattering dependent radiative conductivity tensors in porous media: Application to rod bundles. *Int. J. Heat Mass Transfer*, 52(5-6):1544–1551, 2009.

[13] M. Chahlafi, F. Bellet, F. Fichot, and J. Taine. Radiative transfer within non Beerian porous media with semitransparent and opaque phases in non equilibrium: Application to reflooding of a nuclear reactor. *Int. J. Heat Mass Transfer*, 55(13-14):3666–3676, 2012.

[14] M. Tancrez and J. Taine. Direct identification of absorption and scattering coefficients and phase function of a porous medium by a Monte Carlo technique. *Int. J. Heat Mass Transfer*, 47(2):373–383, 2004.

[15] B. Zeghondy, E. Iacona, and J. Taine. Determination of the anisotropic radiative properties of a porous material by radiative distribution function identification (RDFI). *Int. J. Heat Mass Transfer*, 49(17-18):2810–2819, 2006.

[16] J. Petrasch, P. Wyss, and A. Steinfeld. Tomography-based Monte Carlo determination of radiative properties of reticulate porous ceramics. *J. Quant. Spectrosc. Radiat. Transfer*, 105(2):180–197, 2007.

[17] S. Haussener, P. Coray, W. Lipinski, P. Wyss, and A. Steinfeld. Tomography-Based Heat and Mass Transfer Characterization of Reticulate Porous Ceramics for High-Temperature Processing. *J. Heat Transfer*, 132(2):023305, 2010.

[18] S. Haussener, W. Lipinski, P. Wyss, and A. Steinfeld. Tomography-Based Analysis of Radiative Transfer in Reacting Packed Beds Undergoing a Solid-Gas Thermochemical Transformation. *J. Heat Transfer*, 132(6):061201, 2010.

[19] S. Haussener, W. Lipinski, J. Petrasch, P. Wyss, and A. Steinfeld. Tomographic Characterization of a Semitransparent-Particle Packed Bed and Determination of its Thermal Radiative Properties. *J. Heat Transfer*, 131(7):072701, 2009.

[20] J. Taine, F. Bellet, V. Leroy, and E. Iacona. Generalized radiative transfer equation for porous medium upscaling: Application to the radiative Fourier law. *Int. J. Heat Mass Transfer*, 53(19-20):4071–4081, 2010.

[21] J. Taine and F. Enguehard. Radiative transfer within porous media and couplings. In *Porous media interaction with high temperature and high speed flows*, STO-AVT-261. VKI, 2015.

[22] J. Taine and E. Iacona. Upscaling statistical methodology for radiative transfer in porous media: New trends. *Journal of Heat Transfer*, 134, 2012.

[23] Y. Dauvois. PhD thesis, Ecole Centrale Paris, Grande Voie desVignes, Chatenay Malabry, 92295 cedex, France., 2016 (planned).

[24] S. Torquato and B. Lu. Chord-length distribution function for two-phase random media. *Physical Review E*, 47(4):2950–2953, 1993.

[25] B. Berthet, J. Bonnin, S. Bayle, N. Hanniet, F. Jeury, S. Gaillot, Y. Garnier, C. Martin, M. Laurie, and B. Siri. PHEBUS PF FPT1 - Preliminary Report. DOCUMENT PHEBUS PF IP/97/334, IPSN/DRS/SEA/LERES, Octobre 1997.

[26] X. Jia and X. Williams. A packing algorithm for particles of arbitrary a packing algorithm for particles of arbitrary a packing algorithm for particles of arbitrary shapes. *Powder Technology*, 120:175–186, 2001.

[27] R. Siegel and J. Howell. *Thermal Radiation Heat Transfer*. Taylor and Francis-Hemispher, Washington, 4th ed edition, 2001.